Mixed-effects Model Fitting Based on *in vitro* Data

Borbála Gergics[1,2*], Levente Kovács[1], András Füredi[1,3], and Dániel András Drexler[1]

[1]Physiological Controls Research Center, University Research and Innovation Center, Obuda University, Bécsi út 96/b, 1034 Budapest, Hungary, {gergics.borbala, kovacs, furedi.andras, drexler.daniel}@uni-obuda.hu
[2]Applied Informatics and Applied Mathematics Doctoral School, Obuda University, Bécsi út 96/b, 1034 Budapest, Hungary
[3]Drug Resistance Research Group, Hungarian Research Network, Magyar tudósok krt 2, 1117 Budapest, Hungary, furedi.andras@ttk.hu
[*]Corresponding: gergics.borbala@uni-obuda.hu

Abstract: Personalized therapy optimization in cancer treatment is crucial to improve outcomes and minimize side effects. This study focuses on applying a nonlinear mixed-effects (NLME) model to in vitro tumor spheroid data to better understand tumor growth dynamics and responses to chemotherapy. Tumor spheroids were created using a mammary tumor cell line isolated from Brca1-/-, p53-/- mouse mammary tumors and cytotoxicity measurements were performed with doxorubicin at different concentrations. The NLME model was fitted to longitudinal data sets, capturing both population-level effects and individual variability in tumor growth and drug response. The results suggest that NLME models are highly effective in optimizing therapeutic strategies, taking into account individual tumor characteristics. The study highlights the potential of combining mixed-effects modeling and 3D tumor spheroids to enhance personalized cancer treatment design, ultimately improving treatment efficacy while reducing toxicity.

Keywords: mixed-effects model; therapy optimization; tumor model; in vitro

1 Introduction

Personalized therapies and therapy optimization in chemotherapy are critical for improving patient outcomes and minimizing the side effects and the chance of the development of resistance often associated with cancer treatment. This approach reduces the likelihood of resistance and relapse, as it addresses the unique characteristics of each patient's cancer. Additionally, therapy optimization, which involves adjusting dosage and timing based on patient-specific factors, ensures that treatments are as effective as possible with the fewest side effects [1–4].

The development of mathematical modeling and informatics brings with it the

development of medicine and the engineering support of therapies [5, 6]. Our research focuses on basic research to increase the effectiveness of chemotherapy with the help of mathematical modeling and informatics [7–9]. During basic research in vitro or in vivo biological models are essential for advancing our understanding of tumor function as well as the validation of the built mathematical models and designed therapies [10]. Compared to in vivo animal experiments in vitro biological measurements enable researchers to study biological systems outside of living organisms, providing precise control over experimental conditions and reducing the variability inherent in in vivo studies [11]. Using in vitro methods, scientists can isolate specific variables, conduct high-throughput screening, and perform detailed mechanistic studies, leading to more accurate and reproducible results. Moreover, in vitro measurements play a crucial role in drug development, toxicology, and personalized medicine, allowing for the early identification of potential therapeutic targets and minimizing the ethical concerns associated with animal testing [12–14].

During our work, we create and examine tumor spheroids which are three-dimen-sional cell culture models that closely mimic the architecture and microenvironment of tumors in the human body [15, 16]. Unlike traditional two-dimensional cell cultures, tumor spheroids replicate the complex cell-to-cell and cell-to-matrix interactions found in actual tumors, making them more physiologically relevant for studying cancer biology. These models are particularly valuable for investigating tumor growth, drug resistance, and the efficacy of anti-cancer therapies, as they better reflect the diffusion gradients of oxygen, nutrients, and drugs observed in real tumors. Tumor spheroids also allow researchers to explore the behavior of cancer cells in a more natural state, including their response to treatment, cell migration, and invasion, which are critical for understanding metastasis. As such, tumor spheroids are indispensable tools in cancer research and drug development, offering a more accurate and predictive model for preclinical testing [17–19].

Mathematical modeling of tumors, including tumor cell cultures and tumor spheroids, plays a vital role in understanding tumor growth dynamics, predicting responses to treatments, and optimizing therapeutic interventions. These models offer a quantitative framework to simulate complex biological processes, such as cell proliferation, nutrient diffusion, and drug response, in controlled in vitro environments. In the literature, various tumor growth models range from basic ones using linear dynamics to more complex models that include nonlinear terms in their differential equations. Linear models are easy to work with, but they often fail to capture important biological phenomena. On the other hand, nonlinear models can describe many critical physiological processes, though this increased accuracy often comes at the cost of making the models less practical or more difficult to use [20]. Some of the most commonly used models include the Gompertz and Hahnfeldt models. The Gompertz model [21, 22] is typically applied to describe cancer cell proliferation. On the other hand, the Hahnfeldt model [23] employs non-linear equations to represent the interactions between tumor growth and tumor vascularization.

In longitudinal data, such as cytotoxicity measurements of different chemotherapeutic agents, the variability of observations may grow over time, and repeated measurements from the same individual are correlated. This lack of independence in the data obstructs a key assumption of many statistical methods, which has been largely overlooked in traditional nonlinear models, typically treated as fixed effect models [24]. Non-linear mixed effect models (NLME models) are powerful statistical tools used to analyze complex and variable data by incorporating both fixed effects, which are consistent across all observations, and random effects, which account for variability between different subjects or experimental units [25]. In the context of in vitro data, NLME models are beneficial for capturing the complex and non-linear relationships that often arise in biological systems, such as enzyme kinetics, cell growth dynamics, and drug-response interactions. These models can incorporate the inherent variability between different cell lines, experimental conditions, and replicates, providing a more accurate representation of the biological processes involved [26, 27].

In therapy optimization, NLME models can be used to analyze dose-response relationships, taking into account both the average effect of a drug and the variability in response among different tumor cell populations. This is crucial for identifying optimal dosing regimens that maximize therapeutic efficacy while minimizing toxicity. Furthermore, NLME models can help in predicting how changes in drug concentration or timing may influence tumor growth and treatment outcomes, helping the design of personalized therapy strategies that are tailored to the specific characteristics of a patient's tumor [28, 29]. By integrating data from in vitro experiments with NLME models, researchers can better understand the dynamics of tumor response to therapy, leading to more effective and individualized cancer treatments. In this paper, we present the application of an NLME tumor growth model on data based on in vitro experiments. We created tumor spheroids with the initial cell numbers of 5000 and 10000 cells using a specific mammary tumor cell line. Cytotoxicity measurements were implemented with doxorubicin chemotherapeutic agent, and the model fitting was done on these longitudinal datasets. The model parameters gained from the NLME fitting are the average of the individual estimated parameter values of each spheroid. Thus, the variability of tumor growth and the response to the drug between different individuals can be taken into account.

2 Preliminaries

2.1 Minimal Tumor Model

The applied mathematical model consists of a system of differential equations with four state variables, incorporating both linear components and certain nonlinear terms. This minimal tumor model represents tumor growth, pharmacokinetics, pharmacodynamics, and drug elimination. This system of differential equations can be formulated as follows [30, 31]:

Table 1
The name and dimension of the model parameters.

Parameter	Name	Dimension
a	Proliferation rate	day^{-1}
b	Drug efficiency rate	day^{-1}
n	Necrotic rate	day^{-1}
w	Washout rate coefficient of dead tumor cells	day^{-1}
ED_{50}	Median effective dose of the drug	$\text{mg} \cdot \text{kg}^{-1}$
c	Clearance of the drug	day^{-1}
k1	Flow rate coefficient of the drug from the central to peripheral compartment	day^{-1}
k2	Flow rate coefficient of the drug from the peripheral to central compartment	day^{-1}

$$\dot{x}_1 = (a-n)x_1 - b\frac{x_1 x_3}{ED_{50}+x_3}, \tag{1}$$

$$\dot{x}_2 = nx_1 + b\frac{x_1 x_3}{ED_{50}+x_3} - wx_2, \tag{2}$$

$$\dot{x}_3 = -(c+k_1)x_3 + k_2 x_4 + u, \tag{3}$$

$$\dot{x}_4 = k_1 x_3 - k_2 x_4. \tag{4}$$

The state variables in (1)-(4) describe time-dependent functions. The variable x_1 [mm^3] corresponds to the time function of the living tumor volume, while x_2 [mm^3] represents the dead tumor volume. The drug concentration in the central compartment (the time-dependent drug level in the blood) is given by x_3 [$\text{mg} \cdot \text{kg}^{-1}$], The system input, denoted as u, is the injection rate [$\text{mg} \cdot \text{kg}^{-1} \cdot \text{day}^{-1}$], and this is administered into the central compartment. The time function of the drug concentration in the tissues is described by x_4 [$\text{mg} \cdot \text{kg}^{-1}$]. The model parameters are listed in Table 1.

The drug injections administered on specific days are the model inputs. These doses cause a sudden change in the drug concentration at each injection time. Let t_k, where $k = 0, 1, 2, \ldots$, represent the injection times, and u_k, with $k = 0, 1, 2, \ldots$, be the injected drug doses in $\text{mg} \cdot \text{kg}^{-1}$. As a result, x_3 experiences a discontinuity at time t_k, which is modeled as:

$$x_3(t_k^+) = x_3(t_k^-) + u_k. \tag{5}$$

The model parameters were determined from experiments on mice using a mixed-effects model [30, 31], with the assumption that the parameters remain constant. The objective of this study was to identify and validate these model parameters based on *in vitro* tumor culture data. Although several side effects are not accounted for in the *in vitro* experiments, the impact of chemotherapeutic agents

can be measured more precisely compared to *in vivo* studies, making it easier to incorporate into therapy optimization.

In our previous works, the minimal tumor model was tailored for in vitro experiments, and this modified model was fitted to the entire population of two-dimensional cell cultures or three-dimensional spheroids at once. This fitting did not take into account the individual characteristics of the subjects, so the estimated parameters only provided information about the population average [15, 16, 32].

3 Methods

3.1 Tumor Cell Culture and Spheroid Formation

The cell line used during our work was isolated from Brca1-/-, p53-/- mouse mammary tumors and converted into a stable cell line by researchers from the Drug Resistance Research Group of HUN-REN Research Centre for Natural Sciences. The cell line has a mesenchymal origin and morphology but has a confirmed epithelial background. It divides rapidly, is characteristic of tumor cells, has a doubling time of 34 hours, and exhibits increased motility and genetic instability [33]. The researchers from the HUN-REN Drug Resistance Research Group transfected the genome of the cell line with the green (GFP) fluorescent protein gene, making the cell cultures expressing GFP protein traceable and easier to study with fluorescent microscopy.

To generate spheroids, cells were initially plated in a Poly-HEMA coated 96-well U-bottom plate, with either 5000 or 10000 cells per well. Poly-HEMA, a polymer known for reducing surface adhesion in cell cultures, promotes cell-to-cell adhesion, leading to spheroid formation.

3.2 Cytotoxicty Measurements

Cytotoxicity measurements were taken with the help of JuLI™Stage. The JuLI™ Stage Real-Time CHR (Cell History Recorder) is a fluorescence microscope that can be placed in an incubator and is capable of recording real-time and timelapse recordings of cell cultures, thus enabling their kinetic monitoring [34]. Since it has an automated focus, it is possible to record treatments lasting several days, according to which it records the cell cultures at specific intervals. JuLI™Stage also has an image analysis software capable of recognizing and counting cells based on recordings, so time series measurements of cytotoxicity treatment can also be performed.

After 48 hours of incubation of the cells, the spheroid formation was done and doxorubicin treatment was applied. Doxorubicin is a cytotoxic anthracycline glycoside compound used as a chemotherapy agent, widely used to treat breast

Table 2
Doxorubicin treatment concentration of spheroids belonging to each ID. The ID-s refer the mean values of B, C, and D rows of each column from 2 to 11 in a 96-well plate.

Label ID	Drug conc. (μM)
BCD2	10
BCD3	3.33
BCD4	1.11
BCD5	0.370
BCD6	0.123
BCD7	0.0412
BCD8	0.0137
BCD9	0.00457
BCD10	0.00152
BCD11	0

carcinoma, Kaposi's sarcoma, lymphoma, acute lymphoblastic leukemia, and bladder cancer [35]. The drug was administered using the same serial dilution (10; 3.33; 1.11; 0.370; 0.123; 0.0412; 0.0137; 0.00457; 0.00152; 0 μM) for both 5000 and 10000 initial cell numbers cultures. Data collection was performed over five days using an automated microscope.

The cytotoxicity measurement was conducted in 96- well plates with rows from A to H and columns from 1 to 12. The BCD labels refers to the average values of spheroids treated with the same concentration of doxorubicin in the wells of the B, C and D rows. Drug concentrations were the same in the same column of each row, in descending order from column 2 to 11. The concentrations for each label are summarized in Table 2 The experimental setup was the same for both spheroids with 5000 and 10000 starting cells/well, so the labels of the samples are the same.

3.3 Mixed-effect Model Fitting

The images taken during the cytotoxicity measurement were evaluated using JuLI™ Stage software, called JuLI™STAT. The obtained data was the change of the confluence value of the fluorescence intensity of the area of the image taken from the given well as a function of time. The NLME tumor model was fitted on these experimental data.

The goodness of fit was determined by calculating the individual residual error (IRES), the error between the individual predicted values (IPRED) and the measured data (DV)

$$IRES = DV - IPRED. \tag{6}$$

Initial parameter values need to be defined for the parameter estimation. We used the parameters estimated based on the previous fits [15, 16, 32] on the occasion of

Table 3
Initial parameter values of the model fit on the data of spheroids with 5000 and 10000 initial cells.

Parameter	5000 in. cells	10000 in. cells
a	ln(0.05)	ln(0.45)
n	ln(0.095)	ln(0.48)
b	ln(0.04)	ln(0.01)
ED_{50}	ln(4.48)	ln(4.48)
x_0	ln(1.5)	ln(2.5)

the first run of the NLME fitting. Then, we searched for the best initial values by iteration based on the minimization of the IRES values. The best fit is found at the smallest IRES value, we estimated the model parameters based on this fit.

Table 3 summarizes the initial parameter values in both cases of the fit on 5000 and 10000 initial cell/spheroid datasets.

The fitting results were analyzed in Matlab, while the nonlinear mixed-effects model fitting was carried out in RStudio using the nlmixr2 package. This package is widely used for fitting nonlinear mixed-effects (NLME) models, particularly for pharmacokinetic (PK) and pharmacodynamic (PD) modeling, but is also applicable to other mixed-effects models [36]. SAEM (Stochastic Approximation Expectation-Maximization) estimation algorithm was applied which is a popular method for fitting nonlinear mixed-effects models, especially in pharmacometrics. The SAEM algorithm relies on an iterative process involving the estimation of distributions and data evaluation.

3.4 Tumor Model Tailored to Spheroid Cultures

The minimal mathematical model of tumor growth detailed in Subsection 2.1 was tailored for fitting on in vitro datasets. During the cytotoxicity measurements only the fluorescent intensity of the living cells is measured, we have not got any information about the dead tumor cells, thus (2) is not definable. Furthermore, the drug was added to the system at the beginning of the cytotoxicity measurement, no other drug was added and it was not depleted from the wells during the experiment. Therefore the concentration of the drug (x_3) was not changing and (3) and (4) become invalid during describing the in vitro measurements. Hence the minimal mathematical model of in vitro tumors consists of only the differential equation describing the velocity of tumor proliferation and x_3 was fixed for the measurements of one individual spheroid. As the dead cells were not measured, the necrotic rate (n) of the living cells is not identifiable. For this reason, a new parameter (ϕ) was employed which is the difference between the the growth rate a and necrotic rate n, i.e., $\phi = a - n$. First, we carried out the parameter estimation of the model

$$\dot{x}_1 = \phi x_1 - b\frac{x_1 x_3}{ED_{50} + x_3}. \tag{7}$$

Table 4
The parameters of the modified model

Parameter	Description	Unit
a	Growth rate	1/h
n	Necrotic rate	1/h
ϕ	$a-n$	1/h
b	Inhibition rate	1/h
κ	Hill coefficient	-
ED_{50}	Median effective dose	μM

The results of this fit are detailed in Section 4. During the fitting, it was revealed that at concentrations below 10μM, doxorubicin does not exert a toxic effect on the spheroids. The decrease in fluorescence is primarily the result of drug-free cell necrosis, potential phototoxicity, or the weakening of the fluorophore. This is supported by the parameter values obtained during the fitting summarized in Table 5.

The design of the cytotoxicity protocol and concentration dilution series of the drug is based on the two-dimensional in vitro cell experiments, where concentrations lower than 10μM were also effective. Since during our research, it is also important to see how the three-dimensional spheroids react to the chemotherapy agent compared to the two-dimensional cultures, we used this same dilution series. In order to obtain more detailed information about the effect of the drug at these concentrations, we also estimated the Hill coefficient value during the parameter estimation. Since drug effects are assumed to vary non-linearly with concentration, the Hill function can be used to more accurately describe nonlinear dose-response curves in the study of anticancer drugs. Thus, the phenomenon that the effect increases slowly at lower concentrations, rapidly at intermediate concentrations, and then reaches a plateau phase (saturation) at high concentrations can be mathematically modeled. Thus, our final equation tailored to the in vitro spheroids is described as follows:

$$\dot{x}_1 = \phi x_1 - b x_1 \left(\frac{x_3^{\kappa}}{ED_{50}^{\kappa} + x_3^{\kappa}} \right). \tag{8}$$

The Hill coefficient (κ) is a key parameter in dose-response curves that controls the slope or dose sensitivity of the curve. This parameter basically describes how sensitive a biological system (e.g. cells, receptors) is to changes in the concentration of the active substance. In this work we are investigating which initial Hill coefficient results better fit, thus which estimated Hill coefficient parameter value better describes the reality.

4 Results

During parameter estimation, NLME fitting can help account for the characteristics of the population's fixed effects and the random effects among individuals simultaneously. The fitting was first carried out using the growth model (7), and the results of the parameter estimation based on this can be found in Table 5. Parameters ϕ (difference between a growth rate and n necrotic rate, the Hill coefficient κ, the drug efficiency rate b, the median effective dose ED_{50} and the initial value of fluorescent intensity x_{10} were estimated. It can be seen from the parameters estimated from fitting to (7) that the parameters of the individuals treated with the highest concentration completely distort the parameter averages. This is due to the fact that lower doxorubicin concentrations did not achieve a suitable toxic effect on the spheroids. The decrease in fluorescence of the spheroids indicates drug-free necrosis, phototoxicity, and a decrease in the emission of the fluorophore.

The given concentration series is based on the IC_{50} value of two-dimensional tumor cell cultures, however, we would like to model the effect of the drug on three-dimensional tumor spheroids and estimate the model parameters. Thus, we changed the Hill coefficient, which was initially considered to be 1 in (7), and estimated its value during fitting. This concession from the parameters better described the response of the spheroids to the cytotoxicity measurement, the enormous variability not visible in the estimated toxicity rate (Tables 6-9). The estimated Hill coefficients take on strikingly high values in the case of fitting on measurement data of the initial cell number of 5000 spheroids (Table 6). As κ increases, the response curve of the spheroids to the drug concentration becomes progressively steeper. At such high values, it describes a step function characteristic of a switch. This supports the fact that up to a certain concentration (10μM), doxorubicin does not exert any toxic effect on the spheroids, but from that concentration onward, it almost completely destroys them. Fitting on the cytotoxicity measurement values of spheroids with an initial cell number of 10000 has not caused that high estimated κ values as it is visible from Table 8. This might be due to the higher size of the spheroid and slower drug penetration.

In order to accurately determine the median effective dose (ED_{50}) of doxorubicin for spheroids of this size (with an initial cell number of 5000 and 10000), fine-tuning the concentrations between 10 and 3.333μM is necessary. The median effective dose is located somewhere between these two concentrations. However, based on these results, it can also be established that three-dimensional tumor spheroids respond differently compared to two-dimensional cell cultures and that the half-maximal inhibitory concentration (IC_{50}), which is often confused with ED_{50}, and primarily determined for two-dimensional cells, cannot be appropriately used for spheroids and more complex systems.

In Figures 1-2, the model fitting results are shown. Blue curves represent the measured fluorescence intensity values and red curves mean the predicted values of the NLME fit. Figure 1 shows the fitting results for the cytotoxicity measurement values on spheroids with an initial cell number of 5000, while Figure 2 shows the fitting on the cytotoxicity measurement values on spheroids with an initial cell count

Table 5
Estimated individual parameter values. A minimal tumor model tailored for spheroids was fitted on cytotoxicity measurement values with an initial cell number of 10000, and initial Hill coefficient value $\kappa = 1$.

ID	ϕ	κ	b	ED_{50}	x_{10}
BCD2	-0.022242	1.615442	0.005493	4.268093	2.376880
BCD3	-0.003622	2.332291	0.003432	4.033649	2.164374
BCD4	-0.003120	1.785417	0.001726	4.457707	2.510355
BCD5	-0.004793	1.152972	0.002486	3.945547	2.163662
BCD6	-0.005805	1.595366	0.007443	4.181208	2.107547
BCD7	-0.004874	1.849497	0.006191	4.267777	2.820805
BCD8	-0.004073	1.633602	0.001022	3.953480	2.196299
BCD9	-0.006126	1.855212	0.002431	4.180171	2.468672
BCD10	-0.005403	0.934836	0.001847	4.225823	2.104968
BCD11	-0.008070	0.426864	0.005387	4.191411	2.966651

Table 6
Estimated individual parameter values. A minimal tumor model tailored for spheroids was fitted on cytotoxicity measurement values with an initial cell number of 5000, and initial Hill coefficient value $\kappa > 1$.

ID	ϕ	κ	b	ED_{50}	x_{10}
BCD2	-0.004754	14.858237	0.081815	6.145350	2.055063
BCD3	-0.003575	19.386723	0.070870	6.183408	1.609457
BCD4	-0.002633	13.651719	0.071108	6.188163	1.738363
BCD5	-0.004654	10.899192	0.069790	6.186015	1.572802
BCD6	-0.007163	2.479012	0.068318	6.172896	2.063725
BCD7	-0.006831	9.709235	0.070182	6.140002	1.870437
BCD8	-0.003260	11.176856	0.069749	6.157441	1.688781
BCD9	-0.003635	11.598749	0.071722	6.158471	1.495652
BCD10	-0.004313	10.309986	0.070628	6.146058	1.523355
BCD11	-0.004447	11.455961	0.070667	6.166018	1.660183

of 10000. Both Figures 1 and 2 are divided into ten subplots. Each subplot shows the results of individual tumor spheroids, treated with different concentrations of doxorubicin from 10 μM (left upper subplot) to 0 μM (right bottom subplot). According to Figures 1 and 2,the individual predicted values gained from the fitting of the NLME model closely approximated the real measured values.

The goodness of fit was examined using the individual residual errors (IRES), which is the difference between the predicted and measured values at each measurement point. Table 10 contains the mean and median values of the IRES in all cases. The IRES values were plotted as a function of time, which can be seen in Figures 3-4. The IRES between the predicted and measured value is smaller if the blue dot is closer to the horizontal line of zero, thus the fitting was better.

Table 7
The mean, median, and standard deviation (STD) of the estimated parameters. A minimal tumor model tailored for spheroids was fitted on cytotoxicity measurement values with an initial cell number of 5000, with Hill coefficient $\kappa > 1$.

Parameter	Mean	Median	STD
ϕ	0.0045	0.0044	0.0014
κ	11.5526	11.5526	4.0711
b	0.0715	0.0706	0.0036
ED_{50}	6.1644	6.1622	0.0169
x_{10}	1.7278	1.6745	0.1957

Table 8
Estimated individual parameter values. A minimal tumor model tailored for spheroids was fitted on cytotoxicity measurement values with an initial cell number of 10000. Hill coefficient $\kappa > 1$

ID	ϕ	κ	b	ED_{50}	x_{10}
BCD2	-0.022242	1.615442	0.005493	4.268093	2.376880
BCD3	-0.003622	2.332291	0.003432	4.033649	2.164374
BCD4	-0.003120	1.785417	0.001726	4.457707	2.510355
BCD5	-0.004793	1.152972	0.002486	3.945547	2.163662
BCD6	-0.005805	1.595366	0.007443	4.181208	2.107547
BCD7	-0.004874	1.849497	0.006191	4.267777	2.820805
BCD8	-0.004073	1.633602	0.001022	3.953480	2.196299
BCD9	-0.006126	1.855212	0.002431	4.180171	2.468672
BCD10	-0.005403	0.934836	0.001847	4.225823	2.104968
BCD11	-0.008070	0.426864	0.005387	4.191411	2.966651

Table 9
The mean, median, and standard deviation (STD) of the estimated parameters. A minimal tumor model tailored for spheroids was fitted on cytotoxicity measurement values with an initial cell number of 10000. Hill coefficient $\kappa > 1$

Parameter	Mean	Median	STD
ϕ	0.0068	0.0051	0.0053
κ	1.5181	1.5181	0.5167
b	0.0037	0.0030	0.0021
ED_{50}	4.1705	4.1863	0.1494
x_{10}	2.3880	2.2866	0.2908

Table 10
Mean and median of individual residual errors between the predicted and real measurement values.

Fitting	Mean IRES	Median IRES
5000 in. cells (κ=1)	-0.0048	-0.0069
5000 in. cells ($\kappa > 1$)	-0.0213	-0.0067
10000 in. cells (κ=1)	$-4.3302 \cdot 10^{-4}$	$4.4330 \cdot 10^{-4}$
10000 in. cells ($\kappa > 1$)	-0.0054	$2.2790 \cdot 10^{-5}$

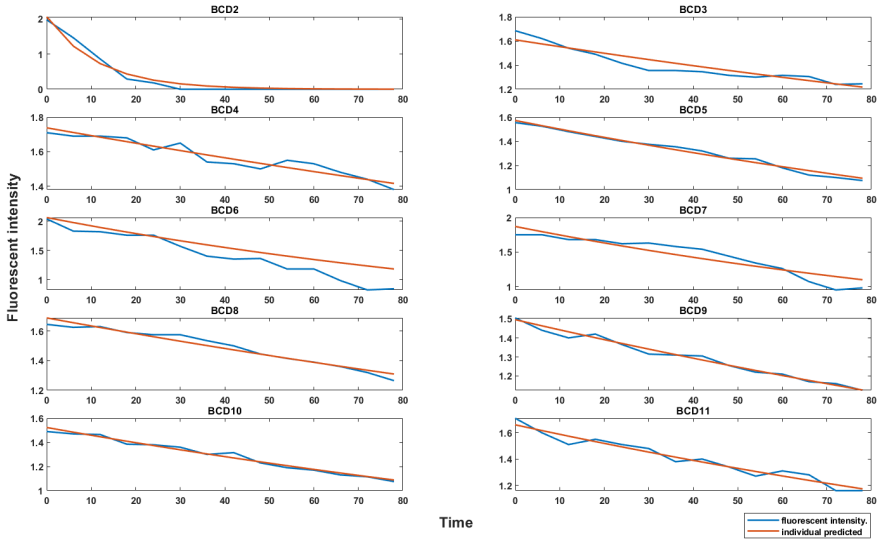

Figure 1
Fitting results for the cytotoxicity measurement values on spheroids with an initial cell number of 5000. A tumor growth model with a higher Hill coefficient ($\kappa > 1$) was fitted on the dataset.

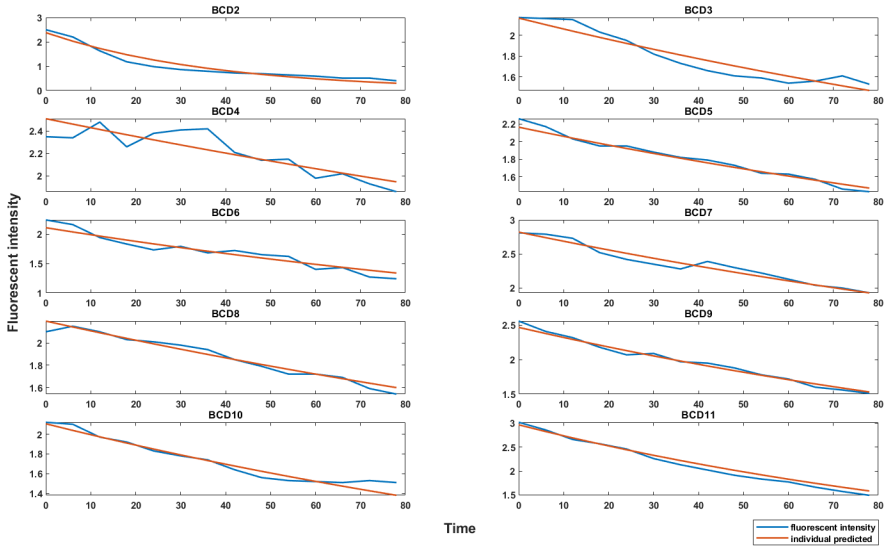

Figure 2
Fitting results for the cytotoxicity measurement values on spheroids with an initial cell number of 10000. A tumor growth model with a higher Hill coefficient ($\kappa > 1$) was fitted on the dataset.

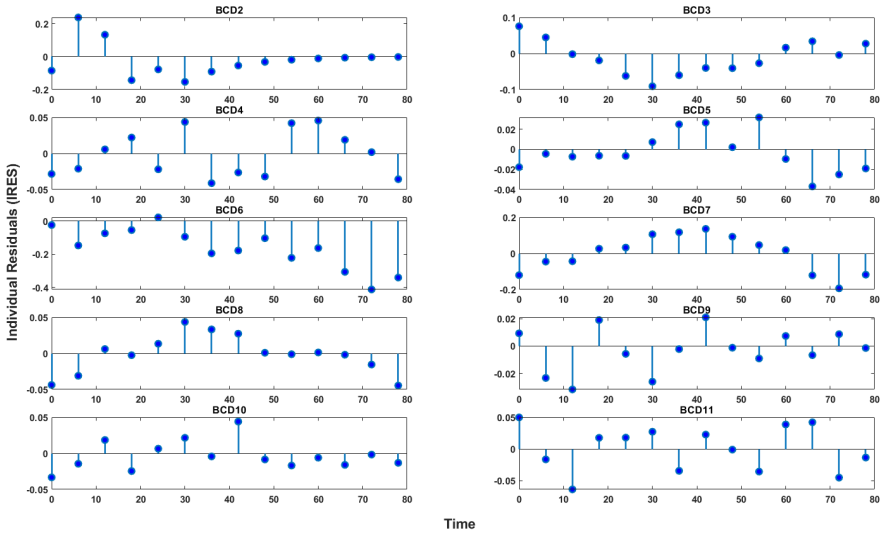

Figure 3
Individual residual errors of the fitted predicted values and the cytotoxicity measurement values on spheroids with an initial cell number of 5000. A tumor growth model with a higher Hill coefficient ($\kappa > 1$) was fitted on the dataset.

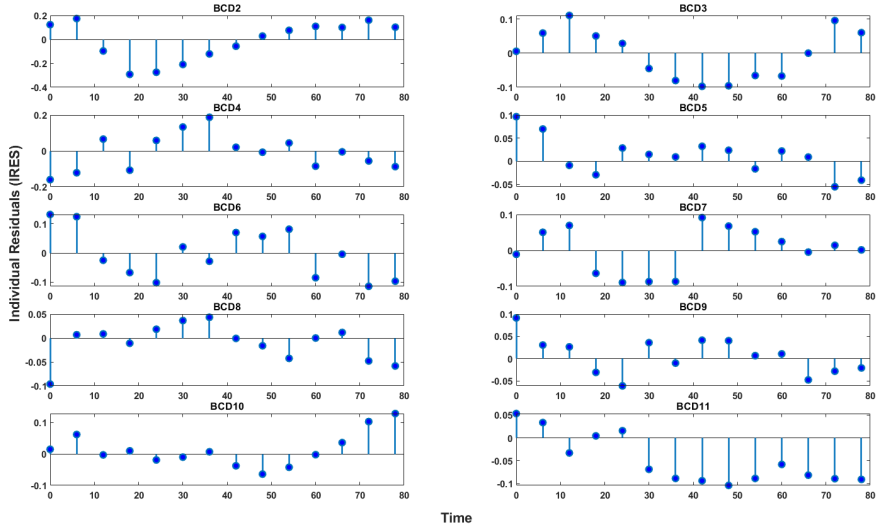

Figure 4
Individual residual errors of the fitted predicted values and the cytotoxicity measurement values on spheroids with an initial cell number of 10000. A tumor growth model with a higher Hill coefficient ($\kappa > 1$) was fitted on the dataset.

Conclusion

The aim of this study was to present and apply a nonlinear mixed-effects (NLME) model based on in vitro data, allowing for more accurate predictions of tumor growth dynamics and responses to drug treatments. The cytotoxicity measurements performed on tumor spheroid models demonstrated that the mixed-effects model successfully fit the real measured values while accounting for the variability between individual cell lines. Throughout the study, the growth dynamics of spheroids treated with different concentrations of doxorubicin were analyzed. Although, in order to accurately determine the median effective dose (ED_{50}) of doxorubicin for spheroids, it is important to fine-tune the concentrations within the range of 10 to 3.333 μM. These findings also highlight that three-dimensional tumor spheroids behave differently from two-dimensional cell cultures and the half-maximal inhibitory concentration (IC_{50}), which is primarily measured for two-dimensional cells, is unsuitable for spheroids or more complex in vivo systems. The results indicated that the model could accurately predict the response of tumor cells to chemotherapy treatments. This confirms that the application of NLME models can be valuable in optimizing therapeutic strategies, allowing for consideration of individual tumor characteristics. Overall, the use of mixed-effects modeling and 3D tumor spheroids represents a promising approach for designing personalized cancer treatments. This method can help maximize treatment efficacy while minimizing toxicity and side effects, ultimately improving patient survival rates and quality of life in the long term.

Acknowledgment

This project has been supported by the Hungarian National Research, Development and Innovation Fund of Hungary, financed under the TKP2021-NKTA-36 funding scheme. The work of Daniel Andras Drexler was supported by the Starting Excellence Researcher Program of Obuda University, Budapest Hungary. Borbala Gergics was supported by the 2024-2.1.1 University Research Scholarship Program of the Ministry for Culture and Innovation from the source of the National Research, Development and Innovation Fund. This research was partially supported by the European Union (EU HORIZON-MSCA-2023-SE-01-01) and the Hungarian NRDI program (2020-2.1.1-ED-2024-00346) within the DSYREKI: Dynamical Systems and Reaction Kinetics Networks project.

References

[1] H. Sbeity and R. Younes. Review of optimization methods for cancer chemotherapy treatment planning. *Journal of Computer Science & Systems Biology*, 8(2):74, 2015.

[2] M. Faruk et al. Breast cancer resistance to chemotherapy: When should we suspect it and how can we prevent it? *Annals of Medicine and Surgery*, 70:102793, 2021.

[3] K. Bräutigam. Optimization of chemotherapy regimens using mathematical programming. *Computers & Industrial Engineering*, 191:110078, 2024.

[4] L. Kovács, T. Ferenci, B. Gombos, A. Füredi, I. Rudas, G. Szakács, and D. A. Drexler. Positive impulsive control of tumor therapy—a cyber-medical approach. *IEEE Transactions on Systems, Man, and Cybernetics: Systems*, 54(1):597 – 608, 2024.

[5] L. D'Orsi, G. Pósfai, and A. De Gaetano. A model of the maldistribution of ventilation and perfusion, in the lungs of heart failure patients. *Acta Polytechnica Hungarica*, 21(9), 2024.

[6] H. Z. Marton, P. E. Inczeffy, Z. Kis, A. Kardos, and T. Haidegger. Results from the study of lesions created by robot-assisted radiofrequency ablation. *Acta Polytechnica Hungarica*, 20(8), 2023.

[7] M. F. Dömény, M. Puskás, L. Kovács, and D. A. Drexler. In silico chemotherapy optimization with genetic algorithm. In *2023 IEEE 17th International Symposium on Applied Computational Intelligence and Informatics (SACI)*, pages 000097–000102. IEEE, 2023.

[8] D. A. Drexler, M. F. Dömény, T. Ferenci, B. Gergics, L. Kisbenedek, M. Puskás, T. D. Szűcs, and L. Kovács. Cyber-medical systems in chemotherapy treatment optimization. In *Recent Advances in Intelligent Engineering: Volume Dedicated to Imre J. Rudas' Seventy-Fifth Birthday*, pages 245–269. Springer, 2024.

[9] L. Kisbenedek, M. Puskás, L. Kovács, and D. A. Drexler. Clustering-based parameter estimation of a tumor model. In *2023 IEEE 21st Jubilee International Symposium on Intelligent Systems and Informatics (SISY)*, pages 000043–000048. IEEE, 2023.

[10] G. Bahcecioglu, G. Basara, B. W. Ellis, X. Ren, and P. Zorlutuna. Breast cancer models: Engineering the tumor microenvironment. *Acta biomaterialia*, 106:1–21, 2020.

[11] C. Zhao. Cell culture: in vitro model system and a promising path to in vivo applications, 2023.

[12] V. Brancato, J. M. Oliveira, V. M. Correlo, R. L. Reis, and S. C. Kundu. Could 3d models of cancer enhance drug screening? *Biomaterials*, 232:119744, 2020.

[13] J. A. Hickman, R. Graeser, R. de Hoogt, S. Vidic, C. Brito, M. Gutekunst, and H. van der Kuip. Three-dimensional models of cancer for pharmacology and cancer cell biology: capturing tumor complexity in vitro/ex vivo. *Biotechnology journal*, 9(9):1115–1128, 2014.

[14] B. Gergics and D. A. Drexler. Mathematical modeling of tumor based on in vitro and in vivo data, and in vitro to in vivo extrapolation and its

challenges: a literature review. In *2023 IEEE 23rd International Symposium on Computational Intelligence and Informatics (CINTI)*, pages 291–298, 2023.

[15] B. Gergics, F. Vajda, M. Puskás, A. Füredi, and D. A. Drexler. Mathematical modeling of phototoxicity during fluorescent imaging of tumor spheroids. In *2023 IEEE 27th International Conference on Intelligent Engineering Systems (INES)*, pages 000291–000296. IEEE, 2023.

[16] B. Gergics, F. Vajda, A. Ládi, A. Füredi, and D. A. Drexler. Pharmacodynamics modeling based on in vitro 3d cell culture experiments. In *2023 IEEE 17th International Symposium on Applied Computational Intelligence and Informatics (SACI)*, pages 000499–000504. IEEE, 2023.

[17] B. Pinto, A. C. Henriques, P. M. Silva, and H. Bousbaa. Three-dimensional spheroids as in vitro preclinical models for cancer research. *Pharmaceutics*, 12(12):1186, 2020.

[18] L.-B. Weiswald, D. Bellet, and V. Dangles-Marie. Spherical cancer models in tumor biology. *Neoplasia*, 17(1):1–15, 2015.

[19] T. Rodrigues, B. Kundu, J. Silva-Correia, S. C. Kundu, J. M. Oliveira, R. L. Reis, and V. M. Correlo. Emerging tumor spheroids technologies for 3d in vitro cancer modeling. *Pharmacology & therapeutics*, 184:201–211, 2018.

[20] J. Sápi, D. A. Drexler, and L. Kovács. Comparison of mathematical tumor growth models. In *2015 IEEE 13th International Symposium on Intelligent Systems and Informatics (SISY)*, pages 323–328. IEEE, 2015.

[21] M. C. Tjørve, Kathleen and E. Tjørve. The use of Gompertz models in growth analyses, and new Gompertz-model approach: An addition to the unified-richards family. *PLOS ONE*, 12(6):1–17, 2017.

[22] C. Vaghi, A. Rodallec, R. Fanciullino, J. Ciccolini, J. P. Mochel, M. Mastri, C. Poignard, J. M. L. Ebos, and S. Benzekry. Population modeling of tumor growth curves and the reduced gompertz model improve prediction of the age of experimental tumors. *PLOS Computational Biology*, 16(2):1–24, 2020.

[23] P. Hahnfeldt, D. Panigrahy, J. Folkman, and L. Hlatky. Tumor development under angiogenic signaling: A dynamical theory of tumor growth, treatment response, and postvascular dormancy. *Cancer Research*, 59:4770–4775, 1999.

[24] S. E. Aggrey. Logistic nonlinear mixed effects model for estimating growth parameters. *Poultry science*, 88(2):276–280, 2009.

[25] M. J. Lindstrom and D. M. Bates. Nonlinear mixed effects models for repeated measures data. *Biometrics*, pages 673–687, 1990.

[26] J. A. Simpson, K. M. Jamsen, T. J. Anderson, S. Zaloumis, S. Nair, C. Woodrow, N. J. White, F. Nosten, and R. N. Price. Nonlinear mixed-effects modelling of in vitro drug susceptibility and molecular correlates of multidrug resistant plasmodium falciparum. *PLoS One*, 8(7):e69505, 2013.

[27] F. Abbas-Aghababazadeh, P. Lu, and B. L. Fridley. Nonlinear mixed-effects models for modeling in vitro drug response data to determine problematic cancer cell lines. *Scientific reports*, 9(1):14421, 2019.

[28] B. Ribba, N. H. Holford, P. Magni, I. Trocóniz, I. Gueorguieva, P. Girard, C. Sarr, M. Elishmereni, C. Kloft, and L. E. Friberg. A review of mixed-effects models of tumor growth and effects of anticancer drug treatment used in population analysis. *CPT: pharmacometrics & systems pharmacology*, 3(5):1–10, 2014.

[29] C. Vaghi, A. Rodallec, R. Fanciullino, J. Ciccolini, J. P. Mochel, M. Mastri, C. Poignard, J. M. Ebos, and S. Benzekry. Population modeling of tumor growth curves and the reduced gompertz model improve prediction of the age of experimental tumors. *PLoS computational biology*, 16(2):e1007178, 2020.

[30] D. A. Drexler, T. Ferenci, A. Füredi, G. Szakács, and L. Kovács. Experimental data-driven tumor modeling for chemotherapy. In *Proceedings of the 21st IFAC World Congress*, pages 16466–16471, 2020.

[31] D. A. Drexler, T. Ferenci, A. Lovrics, and L. Kovács. Tumor Dynamics Modeling based on Formal Reaction Kinetics. *Acta Polytechnica Hungarica*, 16:31–44, 2019.

[32] B. Gergics, B. Gombos, F. Vajda, A. Füredi, G. Szakács, and D. A. Drexler. Pharmacodynamics modeling based on in vitro 2d cell culture experiments. In *2022 IEEE International Conference on Systems, Man, and Cybernetics (SMC)*, pages 2409–2414, 2022.

[33] L. Hámori, G. Kudlik, K. Szebényi, N. Kucsma, B. Szeder, Á. Póti, F. Uher, G. Várady, D. Szüts, J. Tóvári, et al. Establishment and characterization of a brca1-/-, p53-/- mouse mammary tumor cell line. *International Journal of Molecular Sciences*, 21(4):1185, 2020.

[34] Julistage product overview. http://www.julistage.com/product-overview/. Accessed: 2021-11-05.

[35] C. Carvalho, R. X. Santos, S. Cardoso, S. Correia, P. J. Oliveira, M. S. Santos, and P. I. Moreira. Doxorubicin: the good, the bad and the ugly effect. *Current medicinal chemistry*, 16(25):3267–3285, 2009.

[36] Package 'nlme'. https://cran.r-project.org/web/packages/nlme/nlme.pdf. Accessed: 2024-10-01.